Strain rate dependence of the brittle-to-ductile transition temperature in tungsten

Armando Giannattasio, Steve G Roberts

Strain rate dependence of the brittle-to-ductile transition temperature in tungsten

Journal:	*Philosophical Magazine & Philosophical Magazine Letters*
Manuscript ID:	TPHM-06-Nov-0450.R1
Journal Selection:	Philosophical Magazine
Date Submitted by the Author:	18-Jan-2007
Complete List of Authors:	Giannattasio, Armando; University of Oxford, Materials Roberts, Steve; University of Oxford, Materials Science
Keywords:	brittle-ductile transition, crystals, dislocations, fracture, polycrystalline metals, tungsten, plasticity
Keywords (user supplied):	

Strain Rate Dependence of the Brittle-to-Ductile Transition Temperature in Tungsten

A. GIANNATTASIO* and S. G. ROBERTS

Department of Materials, University of Oxford, Parks Road, Oxford OX1 3PH, UK, EU

Abstract

We have investigated the strain rate dependence of the brittle-to-ductile transition (BDT) temperature in pre-cracked tungsten single-crystals and polycrystals. There is an unambiguous Arrhenius relationship over four decades of strain rate, giving an activation energy for the process controlling the BDT of 1.05 eV. This is equal to the activation energy for double-kink formation on screw dislocations, suggesting that their motion controls the brittle-ductile transition.

Keywords: Tungsten; Fracture; Dislocations; Plasticity; Transition

1. Introduction

At low temperatures, body-centered-cubic (bcc) metals generally fail by cleavage and exhibit completely brittle behaviour. At high temperatures, they show typical ductile behaviour, characterized by a marked plastic deformation. A distinctive temperature for this brittle-to-ductile transition (T_{BDT}) can usually be defined for each specific material and test condition.

* E-mail: armando.giannattasio@materials.ox.ac.uk

Metals used for structural applications generally require a low T_{BDT} to minimize the risk of brittle fracture at their operating temperature. Tungsten has been proposed as a plasma-facing metal for critical components in next-generation fusion reactors such as ITER [1] where working conditions would be particularly extreme in terms of radiation damage, high temperatures and stresses. Critical operating conditions (e.g. high strain rates due to thermal shock in a local plasma event) could lead to cracks in the material and thus to catastrophic failure. Hence a basic understanding is needed of the mechanisms controlling the T_{BDT} and its strain-rate dependence in tungsten.

In studies of brittle-ductile transition (BDT) behaviour in single phase (usually single crystal) materials, such as silicon [2], germanium [3], alumina [4], it has been established that the process controlling the BDT is dislocation glide in the region near the crack tip, rather than dislocation nucleation at or near the crack tip. Experimental studies on these materials have shown that the T_{BDT} / strain rate behaviour follows an Arrhenius law with an activation energy equal to that for dislocation glide [2,5]. Dislocation-dynamics models of slip around crack tips and the elastic "shielding" of the crack tip by the active dislocations fit the experimental results to high accuracy [6]. In other materials such as TiAl [7], NiAl [8] and zirconia [9], an Arrhenius law for the BDT with a well-defined activation energy is found, but no data exist for comparison with the thermal activation parameters of dislocation glide. In a study on molybdenum [10], dislocation-dynamics modelling was able to reproduce the variation of fracture stress intensity with strain rate and temperature below the BDT, but was not able to predict the BDT temperature itself. While T_{BDT} depends on strain rate and structure, on a relatively coarse scale it is found for all materials that the ratio between the activation

energy for dislocation mobility, E_v (where $E_v = E_{BDT}$ for the above materials), and T_{BDT} multiplied by the Boltzmann constant, k, is approximately 25 [11].

Gumbsch *et al.* [12] reported experiments on the BDT behaviour of precracked single crystal tungsten using a $\{110\}<1\bar{1}0>$ crack system (i.e. {110} crack plane and $<1\bar{1}0>$ crack front). Three strain rates were used, resulting in loading rates, dK/dt, of 0.1, 0.4 and 1.0 MPam$^{1/2}$s^{-1}; these gave T_{BDT} in the range 300 K to 650 K. From the strain rate variation of T_{BDT}, they deduced an activation energy for the BDT, E_{BDT}, of approximately 0.2 eV. This value is rather lower than the activation energy needed for the glide of screw dislocations (>1 eV) (or, more precisely, for the formation of a kink-pair on a screw dislocation), which control bulk plasticity in tungsten [13,14], and also gives $E_v / kT_{BDT} = 5$. The value of $E_{BDT} = 0.2$ eV could possibly be attributed to the controlling process being the glide of edge dislocations [15,16], since the orientation of the crack system used allows pure edge dislocations to move away from the crack tip on {112} planes in the crystallographic zone of the $<1\bar{1}0>$ crack front. Given a sufficient density of dislocation nucleation sites along the crack front, motion of the associated screw dislocations along the crack front would not be needed to develop a substantial crack tip plastic zone. For other single-crystal orientations and for polycrystalline materials, however, it is unlikely that glide of edge dislocations alone could control the BDT in bcc metals such as tungsten, since expansion of dislocation loops would require motion of slow screw dislocations as well as the fast edge dislocations. Further investigation is needed for a better understanding of the deformation mechanisms controlling the brittle-ductile transition in tungsten.

2. Experimental details

We have investigated the BDT of tungsten using four-point bend testing of precracked single-crystal rectangular bars (1 mm ×1 mm ×11 mm) with sides cut along the <100> directions from an as-grown pure tungsten rod, giving a crack system of $\{100\}\langle 001\rangle$. Similar polycrystalline samples were also studied. Grain size was measured by electron backscattering diffraction (EBSD) analysis of a transverse section, using a local misorientation of >3° to define a grain boundary; the average grain size measured over a total area of 15000μm^2 was determined to be 2.9μm. The pre-cracks, approximately 60 μm deep, were produced on the tensile faces of the bars by using a sharp edge in a spark erosion machine for a few seconds at room temperature; the resulting pre-cracks consisted of a combination of a wedge notch (~20μm deep) and sharp thermally-induced pop in cracks (~40μm deep). Thermally-induced pre-crack planes were mostly (100) and (010) in the single-crystals, whereas in the polycrystalline samples a mixture of inter- and intra-granular pre-cracks was observed. Tests were carried in the temperature range 77 – 550 K and the strain rate range 4×10^{-5} – 5×10^{-2} s^{-1}, giving dK/dt in the range 0.01 – 17 MPam$^{1/2}$s^{-1}. The fracture tests were performed in an argon atmosphere for temperatures above 300K and in a (cooling) nitrogen atmosphere below room temperature. For each sample the surface plastic strain was calculated by subtracting the elastic strain from the total strain. Specimens which fractured with no plastic strain were considered to be fully brittle; those which did not fracture after >5% of plastic strain were considered to be fully ductile; those which fractured in an apparently brittle manner after a limited amount of plastic strain were designated as "semi-brittle" Fracture surfaces of all specimens were examined by optical and scanning-electron microscopy. Figure 1a shows a typical fracture surface of a single-crystal tungsten specimen

tested at 77K; at these low temperatures dislocation activity is expected to be almost completely suppressed and thus brittle cleavage occurs in the material, as indicated by a relatively smooth fracture surface. Figure 1b shows the fracture surface of a similar specimen tested at a temperature close to T_{BDT} (i.e. a semi-brittle specimen). The fracture surface shows clear cleavage; the plastic strain energy is absorbed *before* crack propagation, not *during* crack propagation. Polycrystalline tungsten samples are shown in Figure 2; Figure 2a shows a specimen tested at 77K in which brittle transgranular fracture was found to be dominant. Figure 2b shows a polycrystal sample tested at a temperature close to T_{BDT}; in this case, both brittle transgranular and intergranular fracture can be seen.

3. Results

Figure 3 shows the results obtained with the [001]-oriented single crystal specimens containing {100}<001> crack systems. The low temperature purely brittle fracture toughness, $K_{Ic} = \sigma\sqrt{\pi c}$, where σ is the fracture stress and c is the total crack depth, as measured on each specimen, was found to be (2.7±0.2) MPa m$^{1/2}$, independent of the strain rate. The absence of a strain rate dependence of K_{Ic} at 77K suggests that there is little or no dislocation activity at this temperature. This value is also consistent with that found by Gumbsch [16]. As temperature increases, fracture toughness increases as local plasticity at the crack tip increases. In samples tested at room temperature and above, fracture occurred after macroscopic yielding of the specimen. For comparison, the stress intensity factor at yield, $K_{Iy} = \sigma_y\sqrt{\pi c}$, where σ_y is the measured yield stress, has been plotted in Figure 3 for ductile specimens which did not fail by fracture. The transition from semi-brittle to ductile behaviour occurs

sharply (over <2ºC). The transition temperature T_{BDT} increases monotonically with increasing strain rate, with a variation in T_{BDT} of more than 130°C over the investigated strain rate range.

The results obtained with polycrystalline tungsten specimens are shown in Figure 4. In this case, the measured K_{Ic} at 77K is (4.6±0.3) MPa $m^{1/2}$, double that of the single crystal material. This is probably due to the varied orientation of the small grains which will hinder the propagation of cracks on the lowest-energy {001} fracture planes [17]. In polycrystalline tungsten, as in single-crystals, the fracture toughness increases gradually with increasing temperature up to T_{BDT} for all the strain rates investigated. The values of T_{BDT} measured in polycrystalline tungsten were found to be very close to those observed in single-crystal samples at the same strain rates, although the value of fracture toughness in polycrystals was higher, by a factor approximately two, than that measured in single-crystals at all the temperatures investigated.

Figure 5 shows the experimental T_{BDT} data obtained for both poly- and single-crystals as an Arrhenius plot. In the case of single-crystals, the best fit to the data give an activation energy (1.00±0.04) eV; for polycrystals E_{BDT} = (1.1±0.1) eV. The difference appears not be significant, and combining all data, E_{BDT} = (1.05±0.05) eV. The values of E_{BDT} measured in this work are much larger the 0.2 eV deduced by Gumbsch *et al.* [12].

For four-point bend tests carried out at room temperature and above, the amount of plastic strain at fracture was significant, particularly at temperatures close to T_{BDT} where it increased up to 4.5% in a few cases before cleavage occurred (Figure 6). This indicates that the effects of work-hardening may be important in defining the effective BDT temperature in tungsten. In contrast, only limited plastic relaxation was observed by Gumbsch *et al*. in similar fracture tests on single-crystal tungsten using a three-point bending geometry [12].

At low strain rates (10^{-3} s^{-1} and below) and at temperatures close to T_{BDT}, substantial crack growth was observed in some single crystal specimens. No such crack growth occurred in samples tested at higher strain rates. SEM investigation of the fracture surfaces showed that the crack extended for a few hundred microns before final fast fracture occurred (Figure 7), and that the region of crack growth appeared "brittle" and flat, though with some steps that tended to be aligned along <102> directions. This crack growth is similar to that observed in molybdenum [10] and magnesium oxide [18], where it was thought to be caused by interactions between *anti*shielding dislocations and the crack tip. The mechanism of crack growth in tungsten, from these preliminary results, may play an important role in controlling the BDT at the lower strain rates. This increase in pre-crack length is responsible for the much higher calculated fracture toughness for a few data points at temperatures close to T_{BDT} for low strain rates (Figure 3).

4. Discussion

T_{BDT} at a given dK/dt is not an invariant physical parameter of a material and in general depends on the sample geometry (e.g factors such as relative crack depth, plastic constraint, etc.). Thus, strictly speaking, the data reported here for T_{BDT} in tungsten are only valid for the particular case of the specimen shape and size used in this work. However, although a different geometry of the specimens can be responsible for a shift in T_{BDT} (this corresponds to a change in the pre-factor of the Arrhenius law describing the BDT), such geometrical factors do not produce any variation in the activation energy for BDT. This has been found experimentally in the case of silicon (see, for example, [19]) and also recently predicted by

more general studies on dislocation dynamics (Tarleton and Roberts, unpublished). In addition, recent fracture tests on unnotched tungsten (polycrystalline) bars of the same size as those used in the present work gave a shift in T_{BDT} of approximately -40°C compared with the notched samples, but with no substantial change in E_{BDT} (Giannattasio and Roberts, unpublished).

If the BDT in tungsten is controlled by dislocation velocity, as in other materials, then the likely controlling factor is the mobility of the screw dislocations, since their low mobility compared to edge dislocations [20] implies that screw dislocation motion is the rate-controlling mechanism for the development of dislocation loops and sources. In bcc metals, screw dislocation motion occurs by nucleation and propagation of double kinks along the dislocation line [21]. The rate-controlling factor is likely to be nucleation of kink-pairs rather than their propagation [22].

The enthalpy for kink-pair formation $2H_k$ (at zero stress) in tungsten, for the temperature range investigated in this work, has been measured as $2H_k = 1.75$ eV [13]. According to Seeger's theory of kink-pair formation [21], the thermal component of a resolved shear stress σ^* exerts a repulsive force on the kinks which decreases the value of $2H_k$. An effective kink-pair formation enthalpy H_{kp} (σ^*), which can be identified with the activation enthalpy for screw dislocation motion, can then be written as [22]:

$$H_{kp}(\sigma^*) = 2H_k - 2\alpha\sqrt{\sigma^*}, \quad \text{with } \alpha = (a^3 b\gamma_0 / 2)^{1/2} \qquad (1)$$

where a is the distance between two adjacent Peierls valleys connected by a kink in a dislocation with Burgers vector b and γ_0 is the pre-factor in the logarithmic expression of the dislocation line tension. For tungsten, suitable values are [13] $a = 4.459\times10^{-10}$ m, $\gamma_0 = 9.55\times10^{-10}$ N, and $b = 2.74\times10^{-10}$ m, which give $\alpha = 4.3\times10^{-24}$ $N^{1/2}$ m^2; taking $\sigma^* = 140$ MPa

(this is of the order of the critical resolved shear stress observed in our fracture tests performed between 400K and 500K), a decrease in H_{kp} of 0.64 eV is expected. Equation 1 would then predict H_{kp} = (1.75 - 0.64) eV = 1.11 eV, which is very close to the experimental value of E_{BDT} reported here. In addition, stress-relaxation measurements on tungsten yielded an activation enthalpy for slip between 0.75 eV and 1eV in the temperature range 400-500K [13]. The much lower activation energy (E_{BDT} =0.2 eV) measured in previous experiments by P. Gumbsch *et al.* is probably due to the particular geometry of the $\{110\}<1\bar{1}0>$ crack system investigated in which the crack is mainly shielded by dislocations that are edge in character and thus require a lower activation energy for their motion [15]. In the general case, it is the {100} crack plane which is easiest to activate, as indicated by the similarity of results from polycrystalline tungsten to those from [100]-oriented single crystal specimens. We propose that for {100} cracks in tungsten, crack-tip shielding and/or blunting controls the BDT, and that this is in turn controlled by the motion of screw dislocations which have to overcome an energy barrier of approximately 1 eV in order to glide. This activation energy gives $E_{BDT}/\,kT_{BDT}$ = 25.5 ± 3.6 over the range of strain rates investigated, in good agreement with other materials in which the BDT is controlled by dislocation mobility (see Figure 8).

The dislocation velocity / stress / temperature relation for a given material is a key input parameter for dislocation dynamics modelling of the BDT [6,23]. Currently the only dislocation velocity data available for tungsten are at room temperature and 77K [15], and thus derivation of a sound dislocation velocity law for the experimental temperature range used here is problematic. Work is currently in progress on measuring dislocation velocities in tungsten so as to benchmark such models against experimental data. In terms of practical applications of tungsten in a fusion reactor, though extrapolation of the results reported here

from 77–550K to reactor operating temperatures of 1000-1500K should be treated with caution, such an extrapolation (see Figure 5) indicates that tungsten might be expected to be ductile at such temperatures at strain rates below 10^3 s^{-1}. However, the BDT of tungsten in such applications is likely to be increased by neutron irradiation and by implantation of helium "ash"; further, fracture may result from thermomechanical stresses at lower temperatures in a "cold shut down". Thus the strain rate dependence of the BDT reported here most likely represents a lower bound for brittle conditions.

Acknowledgments

The support of this work by the EU funded project "ExtreMat", contract NMP-CT-2004-500253, is gratefully acknowledged.

References

[1] H. Bolt et al., *J. Nucl. Mater.* **329**, 66 (2004).

[2] S. G. Roberts, J. Samuels, *Proc. R. Soc. Lond.* **A421**, 1 (1989).

[3] F. C. Serbena, S. G. Roberts, *Acta Metall. Mater.* **42**, 2505 (1994).

[4] S. G. Roberts, H. S. Kim, P. B. Hirsch, in *Proc. 9th Int. Conf. on the Strength of Metals and Alloys, Haifa, July 1991*, D. G. Brandon, R. Chaim, A. Rosen, Eds. (Freund, London, 1991) p. 783.

[5] M. Brede, P. Haasen, *Acta Metall.* **36**, 2003 (1988).

[6] P. B. Hirsch, S. G. Roberts, *Philos. Trans. R. Soc. London Ser. A* **355**, 1991 (1997).

[7] A. S. Booth, S. G. Roberts, *Acta Mater.* **45**, 1045 (1997).

[8] H. Vehoff, in *Ordered Intermetallics-Physical Metallurgy and Mechanical Behaviour, NATO Advanced Science Institutes Series, vol. 213 (Series E, Applied Sciences)*, C.T. Liu, R.W. Cahn, G. Sauthoff, Eds. (Kluwer, Dordrecht, 1992) p. 299.

[9] T. J. Marrow, S.G. Roberts, A. K. Pearce-Higgins, *J. Eur. Ceram. Soc.* **14**, 447 (1994).

[10] P.B. Hirsch, A.S. Booth, M. Ellis, S.G. Roberts, *Scripta Metall. et Mater*. **27**, 1723 (1992).

[11] P. B. Hirsch, S. G. Roberts, *Acta Mater.* **44**, 2361 (1996).

[12] P. Gumbsch, J. Riedle, A. Hartmaier, H. F. Fischmeister, *Science* **282**, 1293 (1998).

[13] D. Brunner, *Mater. Trans., JIM,* **41**, 152 (2000).

[14] A. S. Argon, S. R. Maloof, *Acta Metall*. **14**, 1449 (1966).

[15] H. W. Schadler, *Acta Metall.* **12**, 861 (1964).

[16] P. Gumbsch, *J. Nucl. Mater.* **323**, 304 (2003).

[17] J. Riedle, P. Gumbsch, H. F. Fischmeister, V. G. Glebovsky, V. N. Semenov, *Mater. Lett.* **20**, 311 (1994).

[18] A. S. Booth, M. Ellis, S. G. Roberts, P. B. Hirsch, *Mater. Sci. Eng.* **A164**, 270 (1993).

[19] S. G. Roberts, A. S. Booth, P. B. Hirsch, *Mater. Sci. Eng.* **A176**, 91 (1994).

[20] J. P. Hirth, J. Lothe (Editors), *Theory of Dislocations* (Wiley & Sons, New York, 1982).

[21] A. Seeger, in *Dislocations*, P. Veyssiere, L. Kubin, J. Castaing, Eds. (CNRS, Paris, 1984), pp 141-178.

[22] A. Seeger, *Z. Metallkd.* **93**, 8 (2002).

[23] S. G. Roberts, P. B. Hirsch, A. S. Booth, M. Ellis, F.C. Serbena, *Phys. Scripta* **T49**, 420 (1993).

[24] S. Fujita, K. Maeda, S. Hyodo, *Phil. Mag.* **65**, 131 (1992).

[25] P. Pirouz, M. Zhang, J. L. Demenet, H. M. Hobgood, *J. Appl. Phys.* **93** 3279 (2003).

[26] V. I. Trefilov, Y. V. Milman, O. N. Grigoriev, *Prog. Crystal Growth and Charact.* **16** 225 (1988).

[27] K. F. Ha, C. Yang, J. S. Bao, *Scripta Metall. et Mater.* **30** 1065 (1994).

[28] T. D. Joseph, M. Tanaka, A. J. Wilkinson, S. G. Roberts, *J. Nucl. Mater.*, in press (2006).

Figure captions

Figure 1.

Fracture surfaces of single-crystal tungsten material tested at a strain rate of 10^{-2} s^{-1}: (a) test temperature 77K and (b) test temperature 478K (close to T_{BDT}). The smooth surface observed in (a) indicates that dislocation activity has a minor effect at such low temperatures. At high temperatures (b), "river lines" oriented along <110> directions are visible.

Figure 2.

Fracture surfaces of polycrystalline tungsten specimens: (a) test temperature 77K at a strain rate of 5×10^{-2} s^{-1} and at (b) test temperature 419K (close to T_{BDT}) at a strain rate of 10^{-4} s^{-1}. At low temperatures (a), transgranular fracture is dominant; in samples tested at temperatures close to T_{BDT} (b), both intergranular and brittle transgranular fracture are visible.

Figure 3.

Fracture toughness (solid symbols, left axis) measured in single-crystal tungsten as a function of temperature and strain rate. Fracture toughness rises with temperature up to a well-defined transition to ductile behaviour. The transition temperature, T_{BDT}, increases with increasing strain rate. For ductile specimens (no fracture event, open symbols), the stress intensity factor at yield, K_{Iy}, is shown on the right axis.

Figure 4.

Fracture toughness (solid symbols, left axis) measured in polycrystalline tungsten. Open symbols represent ductile specimens. T_{BDT} increases with increasing strain rate. For ductile specimens (no fracture events), the stress intensity factor at yield is shown on the right axis.

Figure 5.

Arrhenius plot of the strain rate versus 1 / T_{BDT} for single-crystal (solid symbols) and polycrystalline (open symbols) tungsten.

Figure 6.

Plastic strain at fracture as a function of temperature for single-crystal tungsten.

Figure 7.

Fracture surface of a [001] single-crystal tungsten sample tested at 4×10^{-5} s^{-1}. Three different regions are clearly visible: (A) a region containing [100]-oriented pre-cracks; (B) an area associated with crack growth, with surface steps aligned mainly along <102> directions; (C) the brittle fast-fracture.

Figure 8.

The activation energy for the BDT as a function of BDT temperature as measured in different materials. Error bars are mainly due to the strain rate dependence of the BDT temperature. Data for W are from this work. Other data are from: Si [2], GaAs [22], Ge [3], Al_2O_3 [4], Mo [10,23], SiC [25], TiAl [7], diamond [26], Fe-3%Si [27], Fe [28], V [28]. The dashed line represents the best linear fit to the data, which gives $E_{BDT} / kT_{BDT} = 25$.

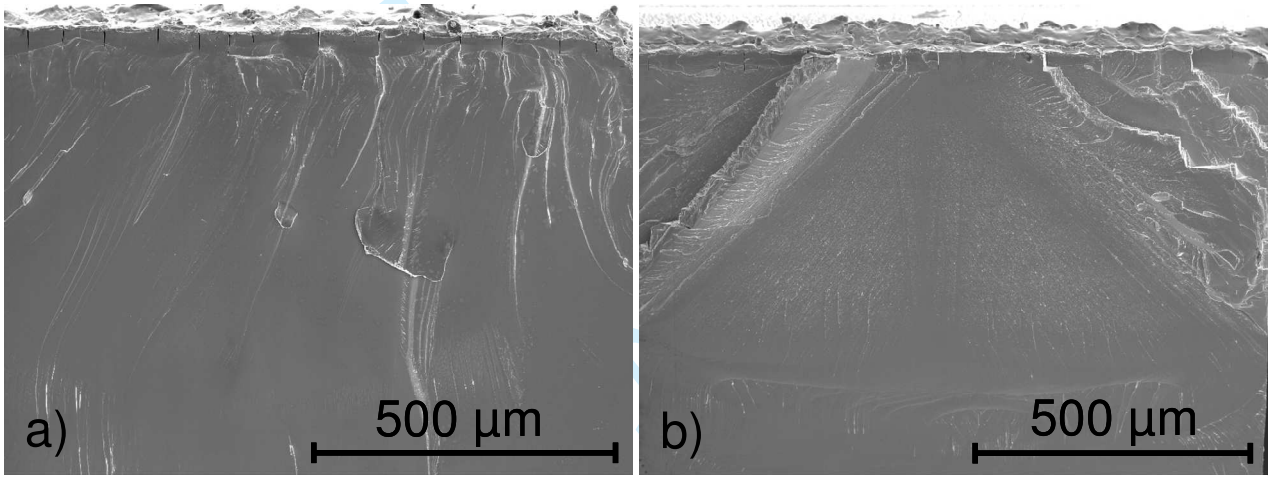

FIGURE 1

Fracture surfaces of single-crystal tungsten material tested at a strain rate of 10^{-2} s^{-1}: (a) test temperature 77K and (b) test temperature 478K (close to T_{BDT}). The smooth surface observed in (a) indicates that dislocation activity has a minor effect at such low temperatures. At high temperatures (b), "river lines" oriented along <110> directions are visible.

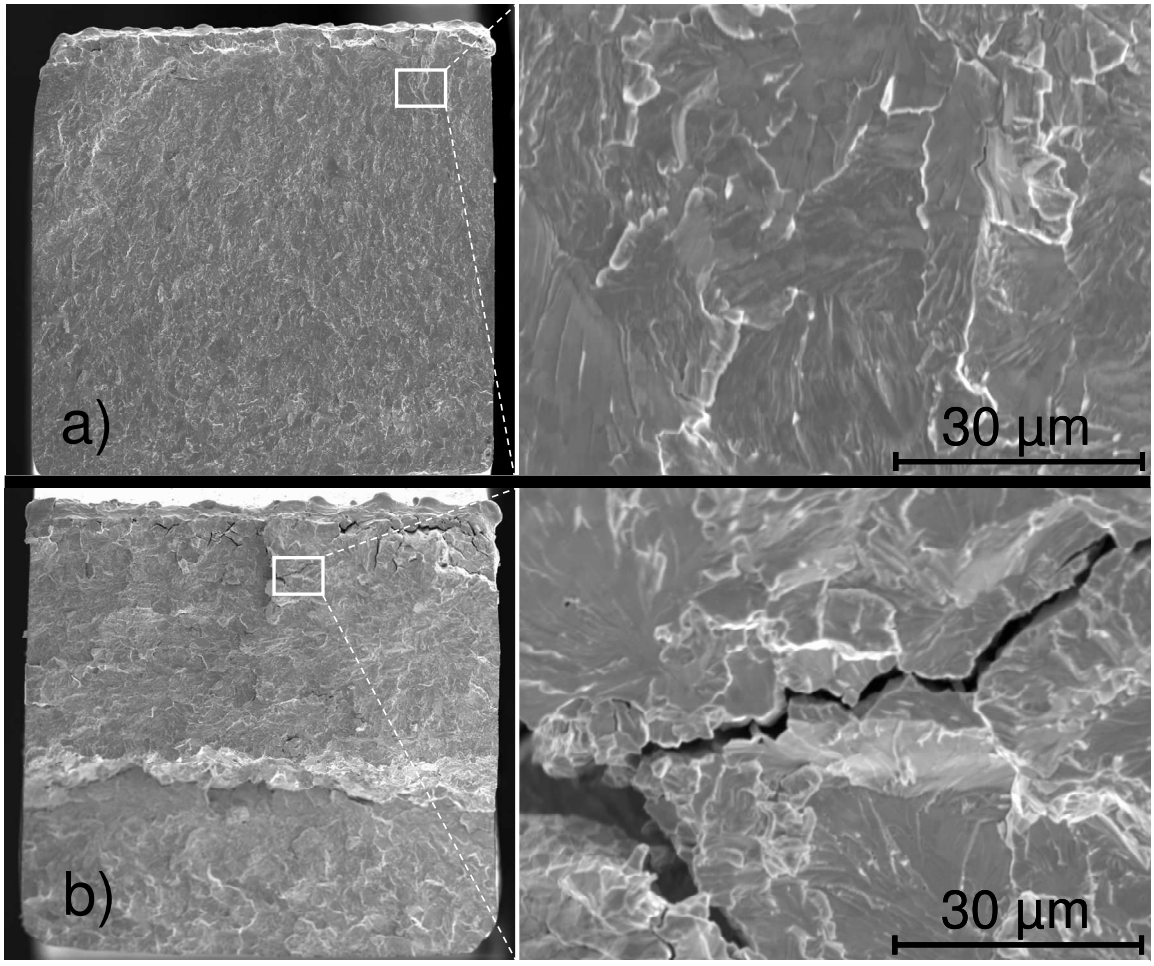

FIGURE 2

Fracture surfaces of polycrystalline tungsten specimens: (a) test temperature 77K at a strain rate of 5×10^{-2} s^{-1} and at (b) test temperature 419K (close to T_{BDT}) at a strain rate of 10^{-4} s^{-1}. At low temperatures (a), transgranular fracture is dominant; in samples tested at temperatures close to T_{BDT} (b), both intergranular and brittle transgranular fracture are visible.

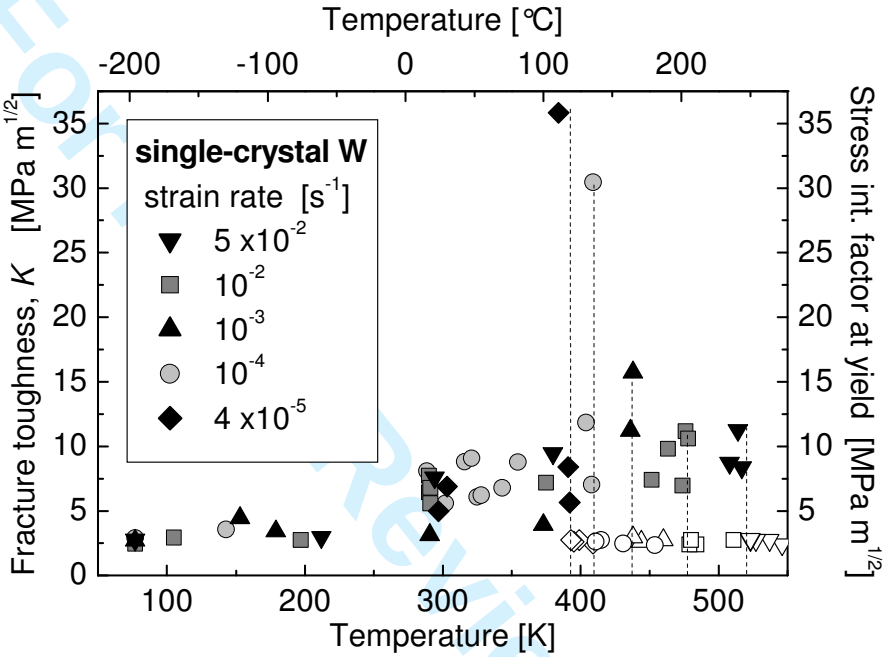

FIGURE 3

Fracture toughness (solid symbols, left axis) measured in single-crystal tungsten as a function of temperature and strain rate. Fracture toughness rises with temperature up to a well-defined transition to ductile behaviour. The transition temperature, T_{BDT}, increases with increasing strain rate. For ductile specimens (no fracture event, open symbols), the stress intensity factor at yield, K_{Iy}, is shown on the right axis.

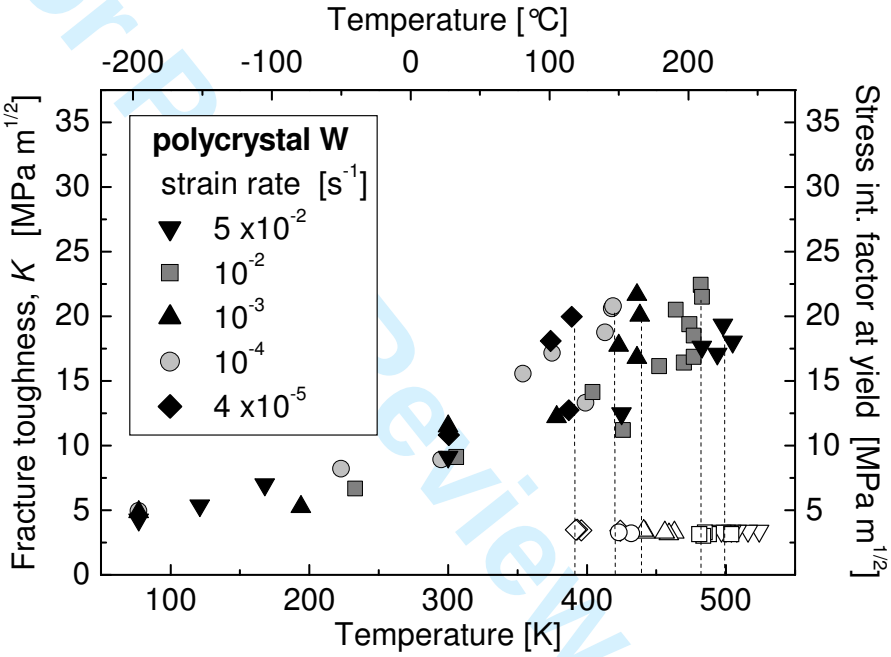

FIGURE 4

Fracture toughness (solid symbols, left axis) measured in polycrystalline tungsten. Open symbols represent ductile specimens. T_{BDT} increases with increasing strain rate. For ductile specimens (no fracture events), the stress intensity factor at yield is shown on the right axis.

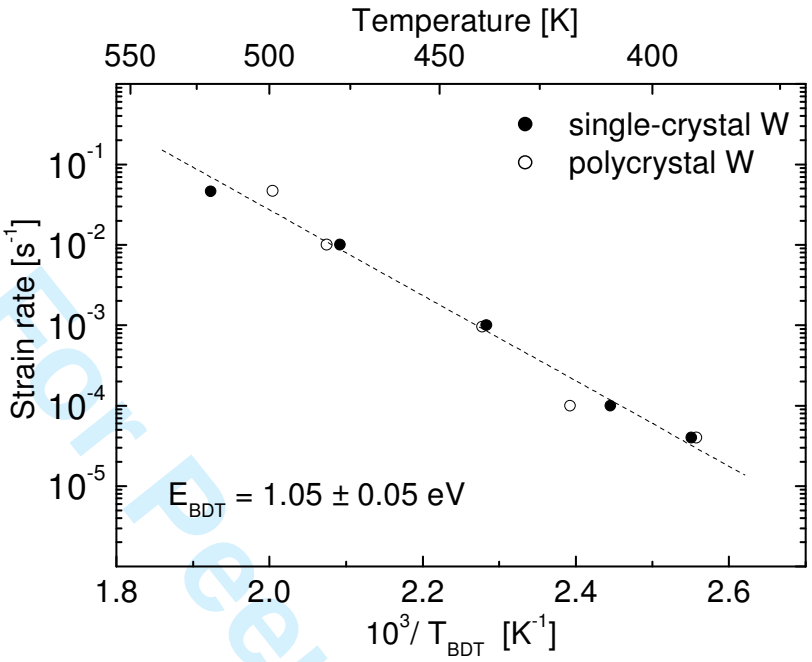

FIGURE 5

Arrhenius plot of the strain rate versus 1 / T_{BDT} for single-crystal (solid symbols) and polycrystalline (open symbols) tungsten.

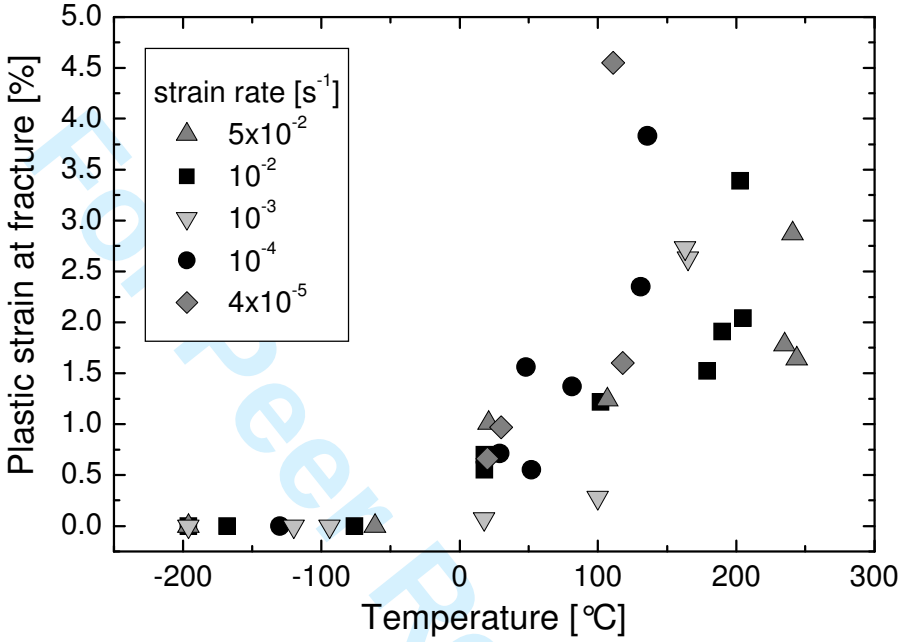

FIGURE 6

Plastic strain at fracture as a function of temperature for single-crystal tungsten.

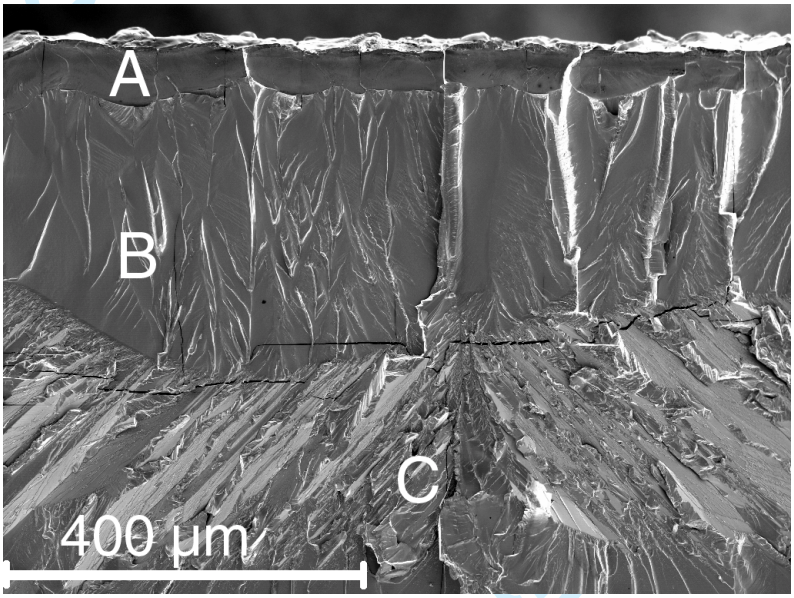

FIGURE 7

Fracture surface of a [001] single-crystal tungsten sample tested at 4×10^{-5} s^{-1}. Three different regions are clearly visible: (A) a region containing [100]-oriented pre-cracks; (B) an area associated with crack growth, with surface steps aligned mainly along <102> directions; (C) the brittle fast-fracture.

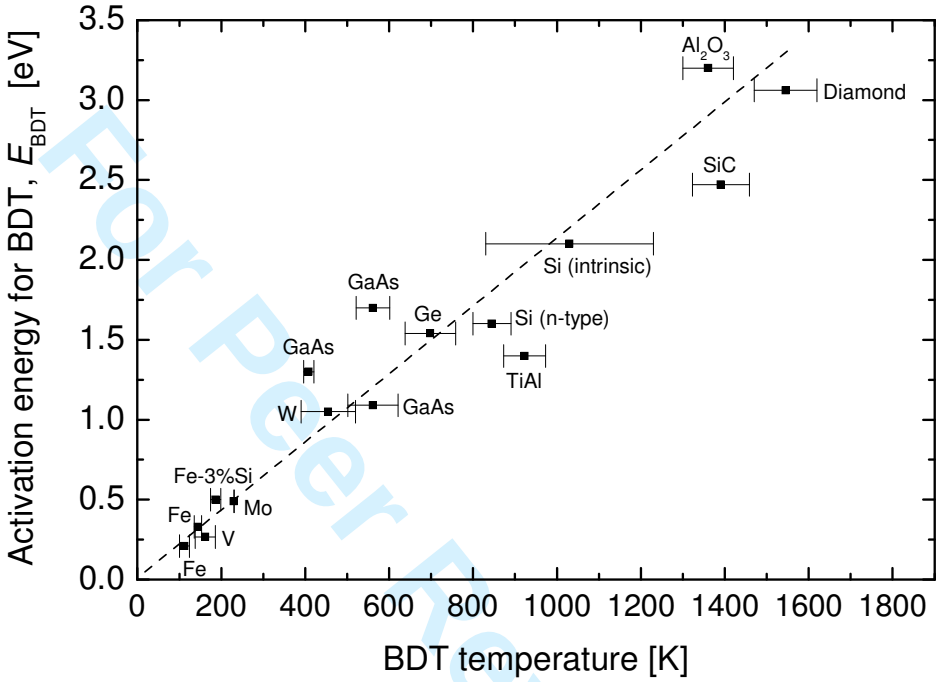

FIGURE 8

The activation energy for the BDT as a function of BDT temperature as measured in different materials. Error bars are mainly due to the strain rate dependence of the BDT temperature. Data for W are from this work. Other data are from: Si [2], GaAs [22], Ge [3], Al_2O_3 [4], Mo [10,23], SiC [25], TiAl [7], diamond [26], Fe-3%Si [27], Fe [28], V [28]. The dashed line represents the best linear fit to the data, which gives $E_{BDT} / kT_{BDT} = 25$.